Journal of Power Sources 303 (2016) 126–136

Contents lists available at ScienceDirect

Journal of Power Sources

journal homepage: www.elsevier.com/locate/jpowsour

Application of current steps and design of experiments methodology to the detection of water management faults in a proton exchange membrane fuel cell stack

Philippe Moçotéguy*, Bastian Ludwig, Nadia Yousfi Steiner [1]

European Institute for Energy Research (EIFER), Emmy-Noether-Str 11, 76131 Karlsruhe, Germany

HIGHLIGHTS

- DoE identifies and puts in order factors impacting water management in PEMFC.
- Two methods are developed to compensate for degradation before DoE analysis.
- Degradation changes factors impacting water management in PEMFC.
- DoE can be used for developing a diagnostic tool for faulty water management.

ARTICLE INFO

Article history:
Received 3 July 2015
Received in revised form
21 October 2015
Accepted 23 October 2015
Available online xxx

Keywords:
PEMFC
Current steps
Dynamic behaviour
Water management
Design of experiments
Fault detection

ABSTRACT

We apply a 2^{5-1} fractional factorial Design of Experiments (DoE) test plan in order to discriminate the direct effects and interactions of five factors on the water management of a 500 We PEMFC stack. The stack is submitted to current steps between different operating levels and several responses are extracted for the DoE analysis. A strong ageing effect on stack and cell performances is observed. Therefore, in order to perform the DoE analysis, responses which values are too strongly affected by ageing are "corrected" prior to the analysis. A "virtual" stack, considered as "healthy", is also "reconstructed" by "putting in series" the cells exhibiting very low performance drop.

The results show that stacks and cells' resistivities are mostly impacted by direct effects of both temperature and cathodic inlet relative humidity and by compensating interaction between temperature and anodic overstoichiometric ratio. It also appears that two responses are able to distinguish a "healthy" stack from a degraded stack: heterogeneities in cell voltages and cell resistivities distributions. They are differently impacted by considered effects and interactions. Thus, a customised water management strategy could be developed, depending on the stack's state of health to maintain it in the best possible operating conditions.

1. Introduction

As the levels of available fossil fuel decrease and as pollutant emissions need to be reduced, alternative energy resources gain more and more attention. Among them, the proton exchange membrane fuel cells (PEMFCs) are one of the most promising candidates for both stationary and automotive applications, as a substitute to traditional systems such as internal combustion engines. They indeed possess several highly advantageous features such as: high efficiency, high power density, low environmental impact, low operating temperature (under 80 °C), simplicity in construction and operation. It can also sustain operation at high current or in discontinuous mode and fast power response at normal temperature [1]. However, their large deployment into the market is still hindered by some issues like low lifetime, reliability and robustness. And, amongst all the related causes, water management is one of the most critical [2,3].

Besides this, due to the rapidly increasing cost of experiments at stack or system levels, efficient experimental approaches are

* Corresponding author.
E-mail addresses: mocoteguy@eifer.org (P. Moçotéguy), ludwig@eifer.org (B. Ludwig), nadia.steiner@univ-fcomte.fr (N. Yousfi Steiner).
[1] Current affiliation: LABEX ACTION CNRS, FEMTO-ST UMR CNRS 6174, FCLAB Research Federation FR CNRS 3539, University of Franche-Comté, rue Thierry Mieg, 90010 Belfort, France.

http://dx.doi.org/10.1016/j.jpowsour.2015.10.078
0378-7753/

Nomenclature

a	DoE coefficient
A	Vector of DoE coefficients
C	Coefficient of dispersion matrix
e	Error
h	Relative humidity [%].
k	Number of factors
N	Total number of experiments
p	Number of DoE model coefficients
r	Number of replicates
s	Overstoichiometric ratio.
t	Time [s]
T	Temperature [K]
U	Voltage [V]
x	DoE equivalent model parameter
X	Design matrix
y	Response value at a given operating condition
Y	Vector of responses

Greek letters

α	Confidence level
β	DoE equivalent model coefficient
ϕ	Heterogeneity in cell resistivity distribution
ρ	Resistivity [$\Omega.m^2$]
σ	Standard deviation
χ	Reduced centred factor
ψ	Heterogeneity in cell voltage distribution

Subscript, superscript

a	Anode
LOF	Lack of fit
PE	Pure error
c	Cathode
corr	corrected
dc	Domain centre
dew	Dew point
exp	experimental
i, j	Identifier number
int	interpolated
η	Double layer capacitance charging
$\bar{}$	Average
$\hat{}$	Estimated

required to minimize the number of runs without sacrificing quality. With this aim, Design of Experiments (DoE) methodology already proved its strong added value in both research and industrial applications. Moreover, this methodology provides an empirical model with studied factors and interactions as parameters that bring additional added value to the experiments. Finally, the underlying statistical and modelling approaches of Design of Experiments facilitate the interpretation of the results, especially for the understanding and the optimization of complex systems [4–8].

As shown in 2009 by Wadhame et al. [9], DoE have already widely been used in the development of materials, components, stacks and even systems performance evaluation. Since then, some other studies used the design of experiments approach for experimental studies of the effect of components manufacturing process [10,11] or nature [12,13] together with cell design [14–16] or operating conditions [13–15,17] on the performances of a PEMFC. Some other studies were also related to the characteristics of the humidifier [18] or reformer [19] on their performance. Finally, some studies aimed, through the approaches underlying the design of experiments methodology, at modelling the performance and behaviour of PEMFC.

Amongst all these studies, only few of them are related to the impact of operational parameters on water management:

- Torchio et al. [20] studied the influence on the electric and thermal powers of a 800 W_e PEMFC stack of some cathodic variables involved in water management: cathodic flow inlet temperature, humidity level and overstoichiometric ratio. They showed that the inlet flow temperature has a significant positive effect on the electric power whatever the current density and that overstoichiometric ratio has a significant positive effect, especially at high-current density on electric power and negative effects on the thermal power. However, humidity level does not have any significant effect on either electric or thermal power, whatever current density level. These results were explained by water flooding in the cathode flow channels.
- Flick et al. [13] discerned and quantified the effect of a microporous layer (MPL) on the impact of water management on the voltage and the cathodic pressure drop in a single cell PEMFC.
- Kahveci et al. [17] optimized the output power density of a 25 cm^2 single cell by studying the effect of reactant flow rates and both operating temperature and humidity level. They found that the humidification and cell temperature are the main factors affecting the power density.

However, none of these works deal with the influence of operational parameters on the effect of water management in the distribution of cell performance and dynamic behaviour of a full stack, as characterized by a high enough data acquisition frequency. Also, none of them applied this methodology to the development of a diagnostic tool.

2. Design of experiments approach

DoE methodology relies on [4–8]:

- Randomization of the experiments order. Both the allocation of the experimental material and the order in which the individual runs are performed are randomly determined. This merges all the sources of variability (uncontrolled or nuisance factors, sensor drift, general background noise in the process, …) within the experimental error.
- Replication of the experiments. This aims at identifying the sources of variability both between runs and potentially within runs and at determining whether the observed differences are statistically significant. Usually, replicates (at very least 3, better 5) are performed at a single standard reference point, which is commonly the domain centre. In such case, the replicates must be regularly spread all along the experimental sequence in order to detect potential "unusual" behaviour: ageing, drift of the response, impact of uncontrolled or nuisance factors during the experimental sequence, …
- The postulate of an a priori empirical Multi Linear Regression (MLR) mathematical model of the response with considered reduced centred factors and interactions as parameters. Its

coefficients correspond to each of their amplitude: the higher the coefficients are, the more influencing the corresponding effects or interactions will be.
- Statistical methods allowing the identification of significant effects and interactions (i.e. model coefficients).

When the number of studied factors increases, the number of experiments needed for the determination of the amplitude of all effects and interactions inflates rapidly. For that reason, interactions with a level higher than two are usually neglected more precisely "aliased" or "confounded" with direct effects or lower level interactions. The abovementioned multilinear regression model is then defined as follow [4–8]:

$$y = \beta_0 + \sum_{i}^{k} \beta_i \cdot \chi_i + \sum_{i}^{k} \left(\sum_{j>i}^{k} \beta_{ij} \cdot \chi_i \cdot \chi_j \right) + e \quad (1)$$

where χ is the value of a reduced centred factor for a given experiment, k is the number of factors, e is the error and the β values are the amplitudes of all the direct effects and interactions to be determined.

This model can also be reformulated as follows:

$$y = a_0 + \sum_{i=1}^{p-1} a_i \cdot x_i + e \quad (2)$$

This gets back to solving a system of at least p equations with p unknowns (one for each coefficient). However, the identification of significant effects and interactions requires the evaluation of the error, e. For that purpose, at least one additional measurement has to be performed, either as replicate of a given operating condition or in any other operating condition within the studied domain. Thus, a system of N (N > p) equations Eq. (2) needs to be resolved. For an easier mathematical resolution of this system, it is formalized in a matricial form [4–8]:

$$Y = X \cdot A \quad (3)$$

where Y stands for the vector of the N observations, X is the matrix containing all reduced centred values χ for each considered experimental condition (also called "design matrix") and A is the vector of the coefficients of the p effects and interactions to quantify.

Special matrix methods aiming at minimizing the least squares estimators in each experimental point are used to estimate the model coefficients. The vector $\hat{A}$ of estimated coefficients is obtained by [4–8]:

$$\hat{A} = \left(X^T \cdot X \right)^{-1} \cdot X^T \cdot Y \quad (4)$$

where:

- X^TX is the "information matrix" and its inverse, $(X^TX)^{-1}$, is the "dispersion matrix". Both are symmetric with dimension (p × p). In case of orthogonality, the matrix is diagonal.
- $(X^T \cdot X)^{-1} \cdot X^T$ is the "alias matrix".
- X^TY is a (p × 1) column vector.

To estimate the significance of the effects and interactions determined by Eq. (4), we assume that model errors follow a normal probability distribution with mean zero and variance, $\sigma^2_{LOF}(y)$. The total variance, $\sigma^2(y)$, is then obtained by adding the lack of fit variance, $\sigma^2_{LOF}(y)$, to the pure error variance, $\sigma^2_{PE}(y)$. The latter is obtained by performing replicates. When replicates are performed in a single point (commonly, the domain centre), it is usually assumed that pure error is constant in the whole domain (homoscedasticity hypothesis) [4,5].

On this basis, the variance of the estimated coefficients in vector $\hat{A}$ is determined by the variance–covariance matrix [4,5,7,21]:

$$\mathrm{Cov}\left(\hat{A}\right) = \sigma^2(y) \cdot \left(X^TX\right)^{-1} \quad (5)$$

The i^{th} main diagonal element of this matrix is the variance of the individual regression coefficient $\hat{a}_i$ and its ij^{th} element is the covariance between $\hat{a}_i$ and $\hat{a}_j$. Under the hypothesis that the experiments are independent (orthogonality), the estimator of all the regression coefficients are uncorrelated and $\mathrm{Cov}(\hat{a}_i, \hat{a}_j) = 0$ (i.e. X^TX is diagonal). Then, the standard deviation of a coefficient is calculated as [5,7]:

$$\sigma(\hat{a}_i) = \sqrt{\sigma^2(y) \cdot C_{ij}} \quad (6)$$

where C_{ij} is the is the ij^{th} element of the dispersion matrix $(X^TX)^{-1}$ corresponding to $\hat{a}_{i,j}$ (the i^{th} diagonal element corresponding to $\hat{a}_i$ in case of diagonal matrix).

To establish the significance of a coefficient $\hat{a}_i$, its value is compared to its standard deviation. It is considered as significant if [4–8]:

$$\left| \frac{\hat{a}_i}{\sigma(\hat{a}_i)} \right| > t_{\frac{\alpha}{2},N-p} \quad (7)$$

where: $t_{\frac{\alpha}{2},N-p}$ is the value of the inverse t-student distribution function with N-p degrees of freedom and α confidence level.

Combination of equations Eq. (6) and Eq. (7) results in:

$$\left| \frac{\hat{a}_i}{\sqrt{\hat{\sigma}^2 \cdot C_{ij}}} \right| > t_{\frac{\alpha}{2},N-p} \quad (8)$$

As a consequence, it results that the $(1-\alpha)$ confidence interval of a_i is given by [4–8]:

$$\hat{a}_i - t_{\frac{\alpha}{2},\,N-p} \cdot \sqrt{\hat{\sigma}^2 \cdot C_{ij}} \le a_i \le \hat{a}_i + t_{\frac{\alpha}{2},\,N-p} \cdot \sqrt{\hat{\sigma}^2 \cdot C_{ij}} \quad (9)$$

3. Experimental

3.1. Set-up

The tested stack was manufactured and designed by the CEA for automotive applications. It had 19 cells with 100 cm^2 active area and contained stamped metallic bipolar plates. It was fed in co-flow and reactant gases entered in cell 1, which corresponds to negative connection. The gases inlet and outlet were on the same side. The "dead end" cell is Cell 19 and corresponds to the positive connection.

The stack was integrated in a test bench which consists of [22]:

- A gas metering system that allows a fine tuning of gas inlet composition from pure hydrogen to simulated reformate as fuel and from pure oxygen to air as oxidant. Gas inlet flow rates can be adjusted up to 110 sL/min for fuel and 330 sL/min for oxidant.
- An Arbin gas humidification system based on gas dew point regulation. The gases were heated up by electric wires all along the distance between the humidification system's outlet and the stack inlet. The tubes inside which the gases flew were

thermally insulated. This aimed at preventing any liquid water condensation between the humidifier and the stack feed-in.
- A Lauda Proline 1845C thermal management system that allows an active cooling and an operating temperature up to 200 °C. It regulates stack temperature with an accuracy of ±0.5 °C.
- A Höcherl & Hackl ZS1606NV electrical load with specific option for an accurate regulation at low current and/or power, able to handle current up to 150 A and power up to 1200 W.
- A Yokogawa WE 7000, able to acquire simultaneously 24 channels at a 100 kHz frequency for 10 s (between 1 s before the step to 9 s after the step).
- A Yokogawa DX2030 data acquisition system with 30 individual channels and an 8 Hz maximal acquisition frequency. The station also has 6 alert channels. Each cell voltage, stack total voltage and pressure drops in both channels were monitored every second.
- Two Rosemount 3051 from Serv'Instrumentation, for pressure drops measurements in each compartment.
- A gas handling system for operating pressure adjustment and with two condensers for trapping water steam from outlet gases.

The whole system is regulated under Labview and regulated parameters are measured at 1 Hz.

3.2. Operating conditions

In a previous review paper, we identified 7 factors that particularly impact water management in a PEM fuel cell [2]:

- Temperature T (°C), of gas entering in both compartments, which also corresponds to stack operating temperature, assuming an inside homogeneous temperature.
- Fuel relative humidity, h_a, defined through entering gas dew point temperature.
- Combustive relative humidity, h_c, defined through entering gas dew point temperature.
- Fuel overstoechiometry, s_a, defined as the ratio between the applied flow rate of hydrogen and the one strictly needed for the electrochemical reaction.
- Combustive overstoechiometry, s_c, defined as the ratio between the applied flow rate of oxygen and the one strictly needed for the electrochemical reaction.
- Operating pressure in both compartments.
- Current density.

Amongst these 7 factors, current density was chosen as a characterization parameter.

Despite its influence on water management, the pressure in both compartments was not considered in this study. Indeed, the stack manufacturer pointed out the harsh operating conditions linked to some combinations of factors values at system level, where the operating pressure is regulated in a narrow window. He therefore recommended to study its effect on a second step and to maintain it at its nominal value, i.e. 1.5 bars in both compartments. This step by step approach is indeed commonly used in design of experiments methodology [5,7,8].

Therefore, only the first five factors were considered in this study. The ranges of variation of each factor was defined according to the specifications of the stack and system manufacturer. These ranges are reported in Table 1 and are mainly linked to operating constraints at system level. Indeed, some combinations of the extrema values of the different factors are incompatible with safety or operability constraints.

In order to minimize the amount of experiments, we chose to leave beside the study of potential quadratic effects and we neglected the influence of interactions having a level higher than two. This results in the necessity to identify 16 coefficients in equation Eq. (2) and this can be performed by a 2^{5-1} fractional factorial design test plan. Moreover, such factorial test plan is orthogonal, which strongly simplifies the mathematical resolution of Eq. (4) [4–8]. The definition of each operating condition is given in Table 2, in which C00 refers to the centre of the domain.

Table 1
Range of variation for studied factors.

Factors	Level −1	Level +1
T (°C)	60	80
h_a (%)	35	75
h_c (%)	35	75
s_a	2	2.5
s_c	2.2	3

The stack was initially stabilized by operating in condition C00 during 24 h before starting the experimental sequence. 11 replicates were performed in the domain centre all along the test campaign. Table 3 correlates the distribution of replicates and the corresponding passed time. A complete analysis of these 11 experiments was presented in a previous paper [22].

Moreover, as recommended for the design of experiments approach and so as to avoid bias effects and merge all the sources of variability within the experimental error, we randomized the experiments order (Cf. Table 4).

3.3. Characterisations

In order to extract some responses used as input for the design of experiments, the stack and each cell were characterized by a succession of current steps, according to profiles similar to the one shown in Fig. 1a. Fig. 1b represents typical current and voltage evolutions resulting from a current step (in this case, from 0.4 A cm^{-2} to 0.2 A cm^{-2}, and measured at a 100 kHz acquisition frequency). It shows the two selected responses for the design of experiments: ohmic resistivity, ρ, and time needed to charge the double layer capacitance, t_η.

So as to prevent any harmful reactant starvation, for each increasing step, flow rate was increased 3–5 s before the current change while, for decreasing steps, flow rate was changed 4–5 s after current change. A minimal flow rate of both reactants gases was also maintained when the cell was left at OCV, in order to

Table 2
Operating conditions.

	h_a (%)	h_c (%)	s_a	s_c	T (°C)
C00	55	55	2.25	2.6	70
C01	35	35	2	2.2	80
C02	35	35	2	3	60
C03	35	35	2.5	2.2	60
C04	35	35	2.5	3	80
C05	35	75	2	2.2	60
C06	35	75	2	3	80
C07	35	75	2.5	2.2	80
C08	35	75	2.5	3	60
C09	75	35	2	2.2	60
C10	75	35	2	3	80
C11	75	35	2.5	2.2	80
C12	75	35	2.5	3	60
C13	75	75	2	2.2	80
C14	75	75	2	3	60
C15	75	75	2.5	2.2	60
C16	75	75	2.5	3	80

Table 3
Correlation between reproduction number in the centre of the domain and "ageing" time.

Replicate n^r	1	2	3	4	5	6	7	8	9	10	11
t (h)	24	72	100	194	220	360	505	700	914	1110	1180

prevent strong reactant starvation at start-up. These flow rates were regulated on the basis of the overstoichiometric ratio to be studied and a current density of 0.1 A cm^{-2}. The consequence of these experimental constraints was that during the few seconds during which the flow rates are readjusted to the new set point values, the actual overstoichiometric ratio changed. However, the current steps were performed at the higher flow rates levels. That's why the overstoichiometric ratio regulated during the design of experiments correspond to the ratio between the current and the flow rates just before the current steps (e.g. for a step down from 0.6 A cm^{-2} to 0.4 A cm^{-2}, the considered overstoichiometric ratio was determined on the basis of an applied current density of 0.6 A cm^{-2}).

- The resistivity determined from the start-up step is about twice as high as the one measured for the other steps. This resistivity was therefore studied as a specific response.
- Except for cell 4, which resistivity increases after 701 h, the cells' resistivities are constant all along the test campaign. The resistivity of cell 4 linearly increased beyond 701 h.
- Response time t_η for step down from 0.2 A cm^{-2} to 0.1 A cm^{-2} varied erratically with high amplitude during the experimental sequence. This step was therefore excluded from the design of experiments analysis.
- For other steps, response time t_η appeared not to be influenced by step level and remained constant all along the experimental campaign. For this reason, the corresponding measurements performed at a given experimental point were considered as replicates.
- During start-up or step up from 0.5 to 0.6 A cm^{-2}, some cells (especially cell 4) went transiently down close to 0 V, or even below. A specific analysis excluding these cells was performed to distinguish a "healthy" stack from a degraded one (Cf. Section 4.2).

4. Data pre-analysis

4.1. Experiments in the domain centre

All the results related to the measurements performed in the centre of the domain are extensively presented in a previous paper [22]. The most relevant results for this study are given below:

- For shut-down steps, a very slow voltage dynamic was observed, preventing any determination of ohmic resistivity and biasing the determination of t_η. This step was therefore excluded from the analysis.
- Except for start-up steps, the level range of the steps has no influence on the resistivity. For this reason, the four corresponding measurements performed at a given experimental point were considered as replicates.

4.2. Data pre-treatment prior to design of experiment analysis

As explained in Section 2, replicates in the centre of the experimental domain are necessary for detecting the presence of a drift, a bias or an ageing effect that could disturb the design of experiment analysis. As shown in our previous paper [22], such an effect was clearly observed. In this case, both Montgomery [5] and Goupy et al. [4] recommend transforming the response so as to get rid of these effects. Such a transformation has the advantage not to affect the properties of the experimental design. For that purpose, two approaches were used:

- Definition of a virtual stack.
- Interpolation of the responses evolutions in the nominal operating conditions and reverse calculation of the "expected" responses values.

Table 4
Correlation between experiment number in Table 2 and time.

Exp	C01	C02	C03	C04	C05	C06	C07	C08	C09	C10	C11	C12	C13	C14	C15	C16
t (h)	48	1100	408	73	1175	170	195	26	1181	240	52	173	50	1090	75	215

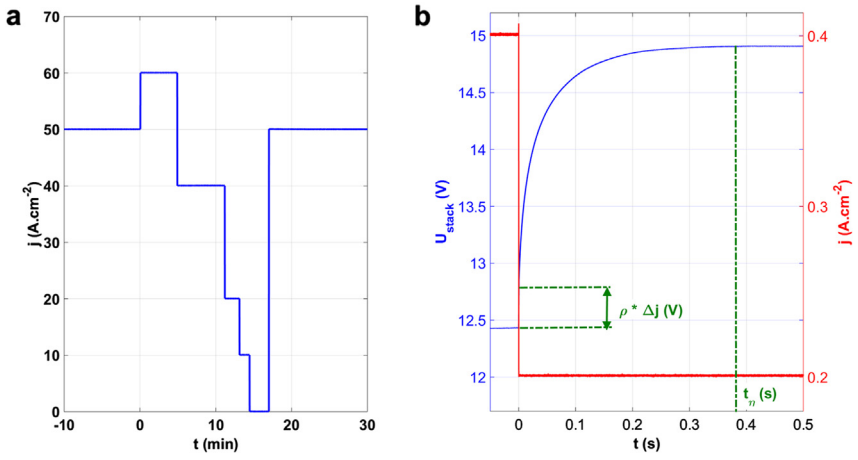

Fig. 1. Typical characterization current profile (a) and extracted responses for the design of experiment (b) (Replicate 5 in the domain centre).

4.2.1. Definition of a virtual "healthy" stack

The evolution of each individual cells' voltage during each current step was recorded in order to determine their resistivity and their dynamic. As mentioned in Section 4.1, in some operating conditions, some cell voltages went transiently to negative values, especially for the start-up step. Such behaviour indicates that they were somehow damaged during the experimental campaign, even if this did not significantly impact their resistivity and their dynamics. Thus, a virtual stack was created. This stack excludes all the cells which voltage went, even transiently, to negative values in at least one step experiment. This reconstructed stack is then considered as still "healthy" after the experimental campaign and was made from cells 5 to 11, 13, 14, 16 and 18 put in series. A resistivity distribution analysis, identical to the one performed for the complete stack has been done and resulting values as been used as response for the design of experiments.

This virtual stack will give us the opportunity to estimate the influence of degradation on the factors impacting water management. In turn, it will give us the possibility to estimate which factors has to be controlled for a water management tool adapted to the actual state of health.

4.2.2. Selected responses

On the basis of these experiments, we considered the following responses for the design of experiments:

- Cell and stack resistivities for all steps except start-up: each experiment was considered as replicated 4 times. In this case, the confidence interval of each coefficient was determined from the variance of the response at each operating point.
- Cell and stack resistivities for start-up step. In this case, the confidence interval of each coefficient was determined from the 11 replicates in the domain centre, assuming that the variance is constant in the whole studied domain (homoscedasticity hypothesis).
- Time, t_η, needed to charge the double layer capacitance for all cells and the stack: each experiment was considered as replicated three times. The confidence interval of each coefficient was determined from the variance of the response at each operating point.
- Heterogeneities in both stacks' cell voltage distribution, ψ, as defined by:

$$\psi = \frac{n_{cell}}{U_{stack}(t=0)} * \sigma(U_{cell}(t)) \tag{10}$$

The confidence interval of each coefficient was determined from the 11 replicates in the domain centre, assuming that the pure error variance is constant in the whole studied domain (homoscedasticity hypothesis).

- Heterogeneities in both stacks' cell resistivity distribution, as defined by:

$$\phi = \frac{n_{cell}}{\rho_{stack}(t=0)} * \sigma(\rho_{cell}(t)) \tag{11}$$

The confidence interval of each coefficient was determined from the 11 replicates in the domain centre, assuming that the pure error variance is constant in the whole studied domain (homoscedasticity hypothesis).

Finally, in addition to the abovementioned "virtual stack", we will also consider for the design of experiments analysis the three first responses at the level of 5 cells clusters (cells 1 to 5, 6 to 10, 11 to 15 and 16 to 19). This aimed at evaluating the possibility to detect degraded cells in the stack while limiting the number of sensors probes.

4.2.3. Responses correction

As mentioned in Section 4.1, cell 4's resistivity showed a break in its evolution with time. Therefore, resistivities measured beyond 701 h of operation were corrected, according to

$$\rho_{4,corr}(t>701h) = \overline{\rho}_{4,C00}(t \le 701h) * \frac{\rho_{4,exp}(t>701h)}{\rho_{4,int}(t>701h)} \tag{12}$$

The interpolation function was empirically determined on the basis of the observed evolution and is defined as follows:

$$\rho_{4,int}(t>701h) = \overline{\rho}_{4,C00}(t \le 701h) + \left(\frac{\rho_{4,C00}(t=1180h) - \overline{\rho}_{4,C00}(t \le 701h)}{479}\right)(t-701) \tag{13}$$

where $\overline{\rho}_{4,C00}(t \le 701h)$ refers to the average value of the resistivities measured in the replicates performed before 701 h of operation.

In addition, as shown on Fig. 2a and b, there is an increase of the heterogeneities in cell voltage distribution with ageing, especially for the real stack (Fig. 2a). In order to correct for the ageing bias effect, we empirically interpolated the evolutions of these distributions, according to the following functions:

$$\begin{cases} \psi_{int,\ real\ stack} = -0.0029 + 0.0147\sqrt{t} - 4.9{*}10^{-4}\cdot t + 5.96{*}10^{-6}\cdot t^{3/2} \\ \psi_{int,\ virtual\ stack} = 0.0018 + 5.14{*}10^{-4}\sqrt{t} - 1.73{*}10^{-5}\cdot t + 2.09{*}10^{-7}\cdot t^{3/2} \end{cases} \tag{14}$$

Then, the actual distributions were corrected according to:

$$\psi_{corr}(t) = \psi(t=0) * \frac{\psi(t)}{\psi_{int}(t)} \tag{15}$$

Their evolutions in the domain centre are respectively represented in Fig. 2c and d, for real and virtual stacks.

5. Results

5.1. Impact of water management on resistivity

The influence of each factor and interaction was determined for each cell's resistivities, using Eq. (4) and their significance was established using Eq. (9). Fig. 3 presents their amplitude for the measurements performed during start-up. Similar results were

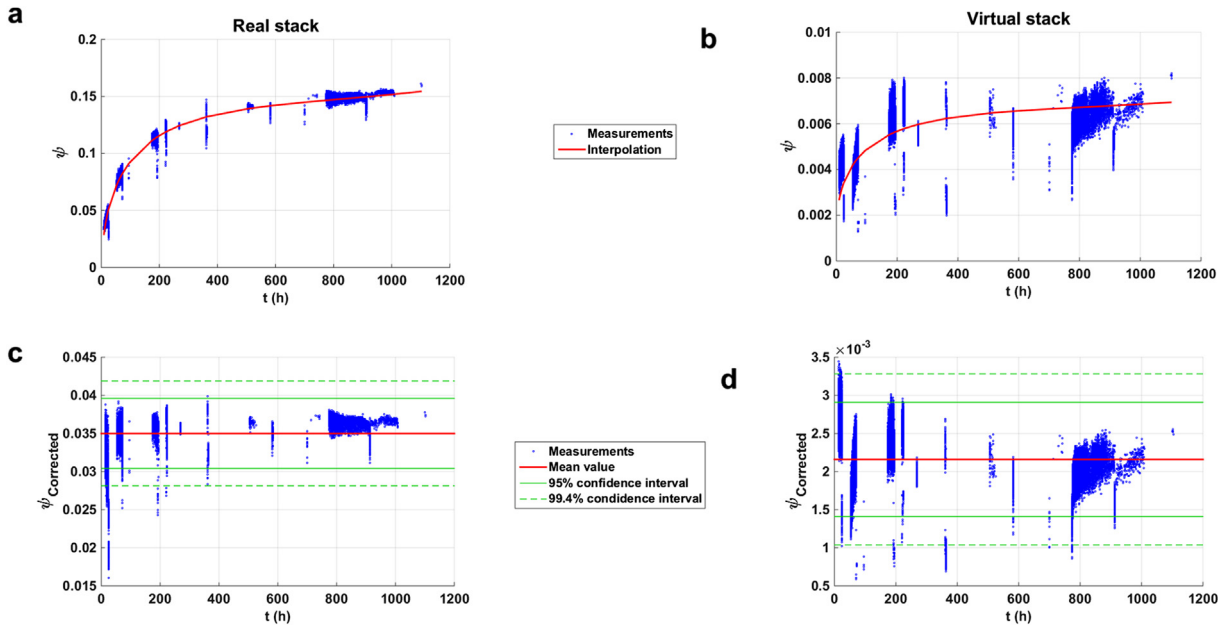

Fig. 2. Evolution with ageing of actual (a, b) and corrected (c, d) values of the heterogeneities of both stacks' voltage distribution.

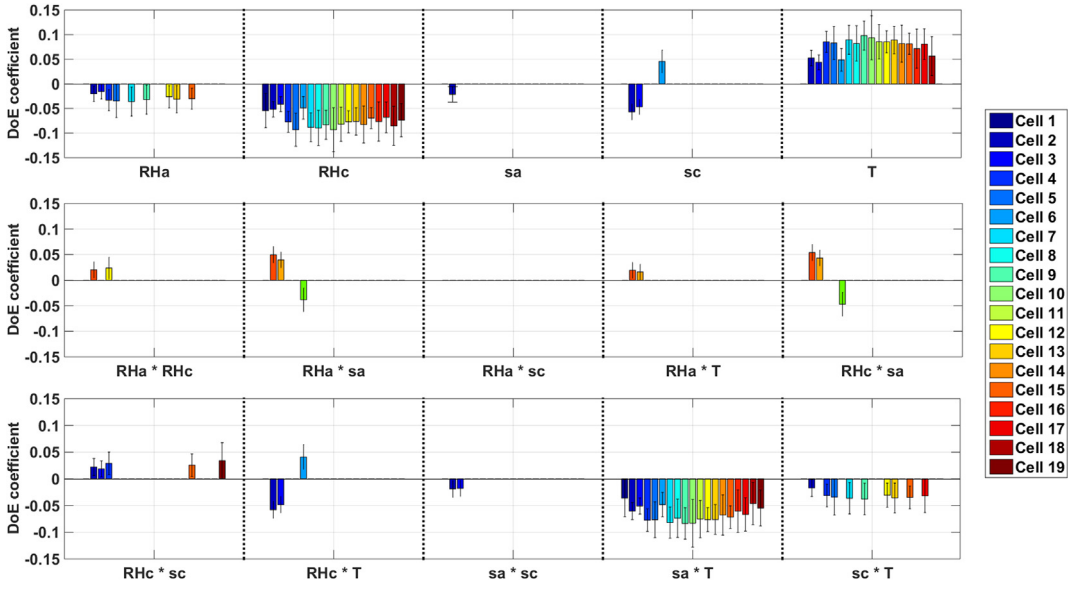

Fig. 3. Distribution of DoE coefficients values for each cell's resistivity response (95% confidence interval).

obtained for the ohmic resistivities determined from the other steps, but their amplitude is ~7 times lower. The figure shows that the cathodic relative humidity, the temperature and the compensating interaction between temperature and anodic overstoichiometric ratio are the most impacting parameters on ohmic resistivities. For both real and virtual stacks, their cumulated impact on the resistivities represents ~60% to ~80% of the total impact.

Fig. 3 shows that a decrease in relative humidities and an increase in temperature result in higher ohmic resistivities, most probably related to MEA drying. It also appears that the sensitivity to factor variations is lower in the first cells, which might be explained by a higher humidity at gas inlet. We also notice that for significant coefficients involving temperature, the resistivity evolution follows a bell (or inversed bell) shape from feed end to dead end. A possible explanation could be that more heat is produced in the heart of the stack increasing the actual temperature.

Then, we compared the influence of each factor and interaction on the resistivities of both stacks and of each cluster. No significant difference was observed between the results obtained for both stacks and each cluster (not shown here). At stack or cluster scales, degradation cannot be detected by the analysis of ohmic resistivity. Therefore, for the resistivity response, stack clusterisation does not present any added value for diagnostics purpose.

Fig. 4 compares the DoE coefficient values calculated for the heterogeneity in cell resistivity distribution for both real and virtual stacks. It can be observed that:

- Heterogeneities in the virtual ("healthy") stack are about ten times lower than for the real (degraded) stack.
- The impacting factors and interactions are different for both stacks. Even if some common impacting effects and interactions

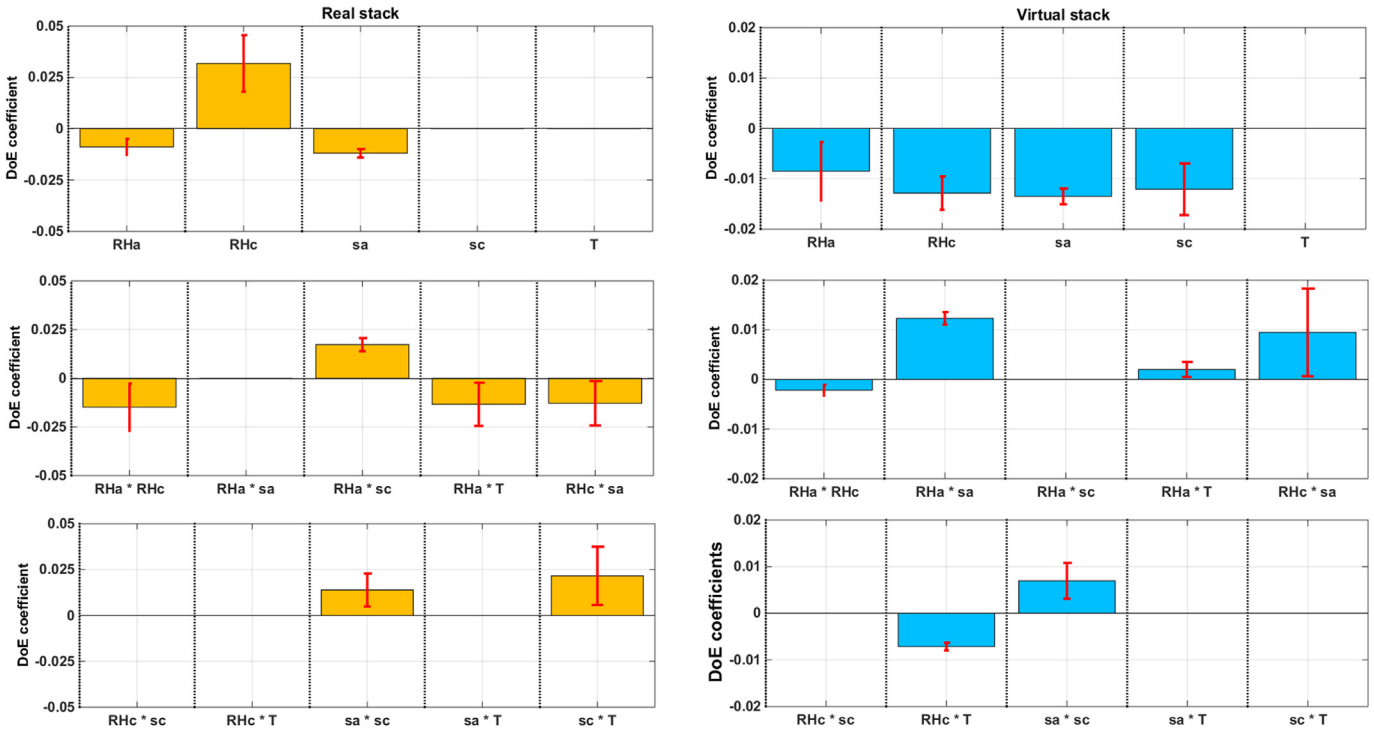

Fig. 4. Comparison between DoE coefficients values for the heterogeneity in cell resistivity distribution for both real (left graphs) and virtual (right graphs) stacks (95% confidence interval).

exist, their impacting amplitude is significantly different and their influences are in some cases opposite (e.g. direct effect of cathodic relative humidity).

5.2. Impact of water management on cells' dynamics

The influence of each factor and interaction was determined for each cell's dynamic, using Eq. (4) and their significance was established using Eq. (9). Fig. 5 represents the distribution within the stack of DoE coefficients obtained for the time needed to charge the double layer capacitance, with a significance probability of 95%. From this graph, it appears clearly that, for most cells, the only significant factor is temperature. However, the cells located at gas inlet are more sensitive to variation of other factors and interactions, either in amplitude or versus the number of coefficients. These cells also correspond to the most degraded ones. A similar analysis was made at stacks and clusters levels: the dynamics of real stack and cluster 1 are the most sensitive to water management while the dynamic of the virtual stack, which only contains the "healthy" cells, is not significantly impacted by water management.

Therefore, the more the stack is degraded, the more its

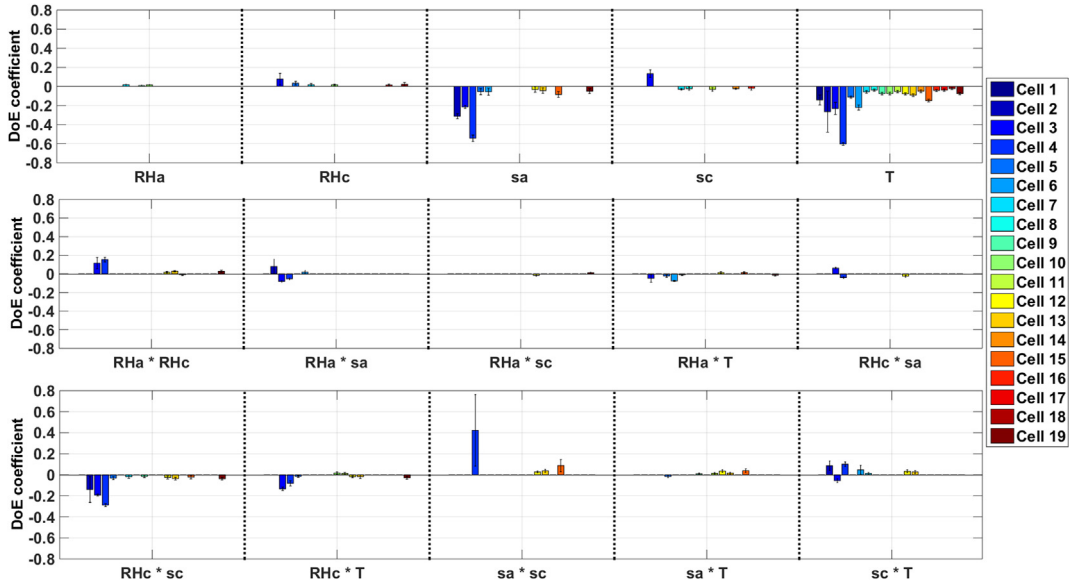

Fig. 5. Distribution of DoE coefficients values of the time needed to charge each cell's double layer capacitance (95% confidence interval).

dynamics are sensitive to water management and mainly to 5 factors and interactions: temperature, anodic overstoichiometric ratio and interactions between cathodic relative humidity and overstoichiometric ratio, cathodic overstoichiometric ratio and temperature and both overstoichiometric ratio.

5.3. Impact of water management on the heterogeneities in cell voltage distribution

Fig. 6 compares the DoE coefficient values calculated, using Eq. (4), for the heterogeneity in cell voltage distribution for both real and virtual stacks. Their significance was established using Eq. (9). A first direct observation shows that the heterogeneity of cell voltage distribution in the virtual stack is about ten times lower than for the real stack. We can also notice that the factors and interactions that impact the cell voltage distribution are different for both stacks and even that, if it exists some common impacting effects and interactions, their impacting amplitude is significantly different and they can even be opposite. This is for instance the case for the direct effect of cathodic relative humidity and for the interaction between both overstoichiometric ratios. The former is positive with a high impact for the real stack and negative with a lower impact for the virtual one while the latter is synergistic with a limited amplitude for the real stack and compensating with a high amplitude for the virtual stack.

5.4. Detection of potential quadratic effects

As recommended in the literature [4–8], the replicates in the domain centre were used to segregate lack of fit error from pure (experimental) error. The former is linked to the inability of the model in Eq. (2) to estimate the value in the domain centre while the latter is linked to the intrinsic variability of the measurements performed in the domain centre. For each cell, each stack and each cluster, the average and 95% confidence intervals of estimated and experimental values in the domain centre were determined.

The average of estimated value in the domain centre corresponds to a_0 in Eq. (1) and Eq. (2). Each confidence interval for each value was estimated according to [4–8]:

$$\sigma_{PE} = \sqrt{\frac{\sum_{i=1}^{r_{dc}} \left(y_{i,dc} - \overline{y}_{i,dc}\right)^2}{r_{dc} - 1}} \tag{16}$$

$$\sigma_{LOF} = \sqrt{\frac{r_{dc} \cdot \left(\overline{y}_{i,dc} - a_0\right)^2}{r_{dc} - 1}} \tag{17}$$

Fig. 7 compares both experimental and estimated ohmic resistivities in the domain centre for each cell and for each stack and clusters. The graphs show that, whatever the cell number, the cluster number or the stack state of health, both values are statistically identical. This indicates that no significant quadratic effect is present in the studied domain. Same results (not shown here) were obtained for ohmic resistivities at start-up and for the dynamic.

As far as the cell voltage distribution is concerned, besides the DoE operating conditions, measurements are available on 23 additional operating points inside the studied domain. These measurements are obtained in stable conditions and are linked to the experimental constraints associated with the test bench regulation, which makes us change one (maximum two) factor simultaneously and sometimes by steps. These additional conditions allowed us to evaluate the validity of the model inside the domain by comparing, for each condition, the experimental value with the one estimated by the model. As shown in Fig. 8, both values are significantly different. In some cases, for the virtual stack, the estimated value is even negative, which is a non-sense for a distribution's heterogeneity. This clearly indicates the presence of quadratic effects for the cell voltage heterogeneity response within

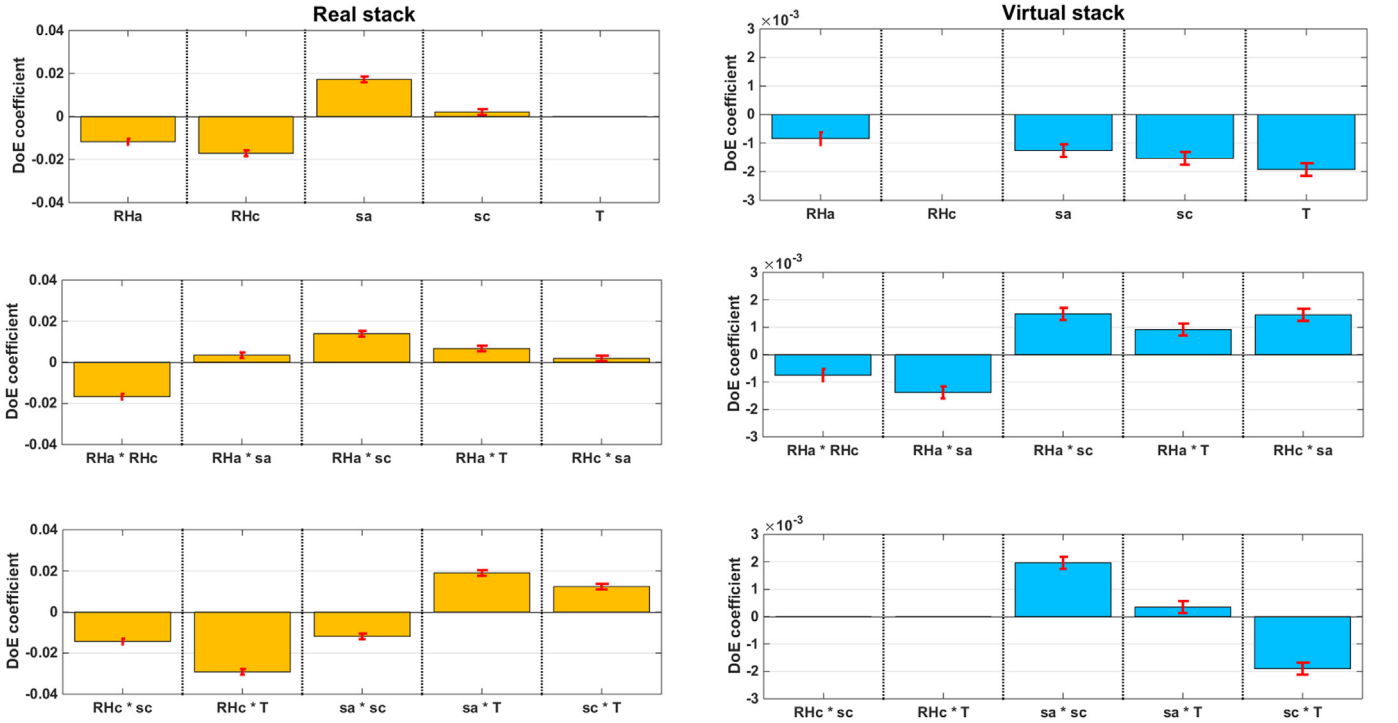

Fig. 6. Comparison between DoE coefficients values for the heterogeneity in cell voltage distributions for both real (left graphs) and virtual (right graphs) stacks (95% confidence interval).

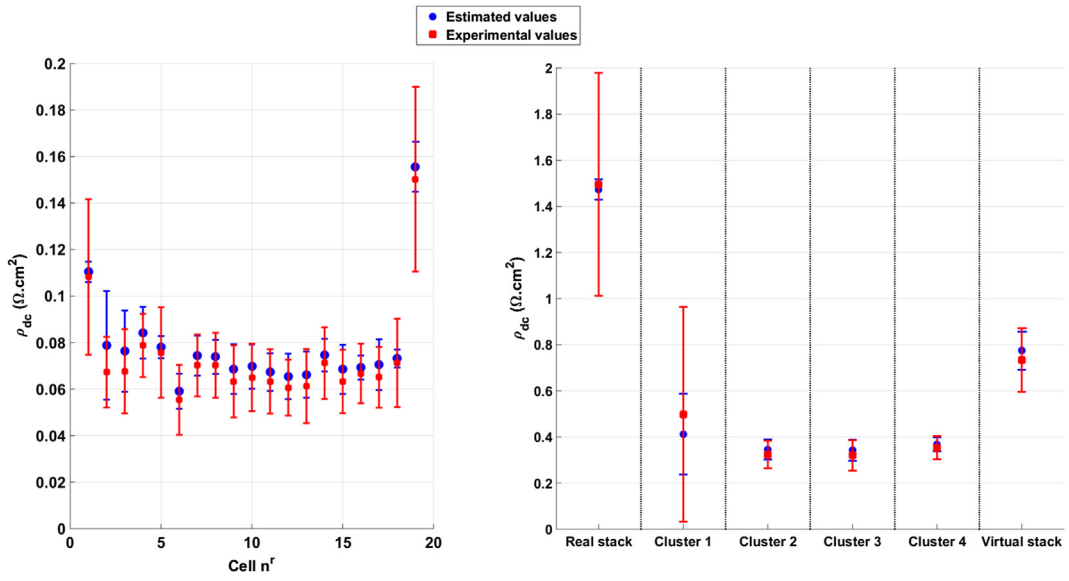

Fig. 7. Comparison between estimated and experimental resistivities in the domain centre.

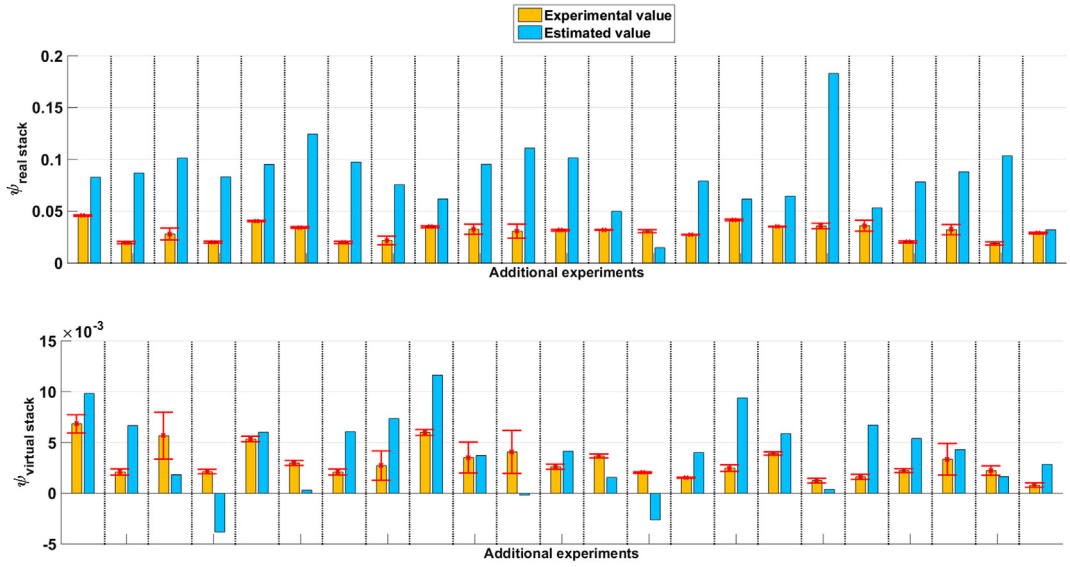

Fig. 8. Comparison between experimental and estimated heterogeneity in cell voltage distribution for real (upper graph and virtual (bottom graph) stacks.

the studied domain.

6. Application to diagnostic

From the results presented above, it appears that two indicators can be used to distinguish a “healthy” stack from a degraded one: the heterogeneities in both cell voltage and resistivity distributions. Table 5 summarizes the significant effects' direction for these two responses for both real and virtual stacks. This table shows that factors and interactions to which the two responses are sensitive are different for both stacks. Using these two responses, a degraded stack can thus be distinguished from a “healthy” one.

A deeper analysis of the evolutions of these responses vs. the operating factors and their interactions could therefore pave the way of the development of a customised water management strategy. This would allow the operation in the best possible operating conditions.

7. Conclusions

During this study, design of experiment methodology was used for studying the impact of several factors and their interaction on the water management of a PEMFC stack. To cope with the observed ageing effects, a specific protocol based on responses correction (defined through the interpolation of the performances evolution in the domain centre) and a virtual stack reconstruction was developed. The virtual stack integrated cells which performances were negligibly impacted by ageing. The sensitivities of both real (considered as degraded) and virtual (considered as “healthy”) stacks to the variations of factors and interactions were compared. The results showed that, whatever the stack's state of health, the factors and interactions impacting the resistivity are identical: there is a direct negative effect of temperature (the higher it is, the lower the resistivity is), a direct positive effect of cathodic relative humidity and a compensating interaction

Table 5
Comparison between DoE coefficients' signs for the two selected responses for both real and virtual stacks (N.S. = non significant).

Factor/interaction	Cell voltage distribution		Cell resistivity distribution	
	Real stack	Virtual stack	Real stack	Virtual stack
h_a	<0	<0	>0	N.S.
h_c	<0	N.S.	>0	<0
s_a	>0	<0	N.S.	N.S.
s_c	>0 (~-negligible)	<0	N.S.	<0
T	N.S.	<0	N.S.	>0
$h_a \times h_c$	<0	<0	<0	N.S.
$h_a \times s_a$	>0 (~-negligible)	<0	N.S.	>0
$h_a \times s_c$	>0	>0	>0	N.S.
$h_a \times T$	>0	>0	N.S.	N.S.
$h_c \times s_a$	>0 (~-negligible)	>0	<0	N.S.
$h_c \times s_c$	<0	N.S.	N.S.	N.S.
$h_c \times T$	<0	N.S.	N.S.	<0
$s_a \times s_c$	<0	>0	N.S.	N.S.
$s_a \times T$	>0	>0 (~-negligible)	>0	<0
$s_c \times T$	>0	<0	>0	<0

between anodic overstoichiometric ratio and temperature. Amongst the several other responses, two were able to distinguish the "healthy" stack from the degraded one: the heterogeneities in cell voltage and resistivity distributions.

A deeper analysis of the evolutions of these responses vs. the operating factors and their interactions could therefore pave the way for the development of a faulty water management detection tool. This would allow the operation in the best possible humidity conditions, which could extend the stack lifetime.

Acknowledgement

The authors would like to thank the French Research National Agency for having funded this work (ANR-06-PANH-0004).

References

[1] J. Larminie, A. Dicks, Fuel Cell System Explained, first ed., John Wiley & Sons, 2000.
[2] N. Yousfi-Steiner, P. Moçotéguy, D. Candusso, D. Hissel, A. Hernandez, A. Aslanides, J. Power Sources 183 (2008) 260–274.
[3] H. Li, Y. Tang, Z. Wang, Z. Shi, S. Wu, D. Song, J. Zhang, K. Fatih, J. Zhang, H. Wang, Z. Liu, R. Abouatallah, A. Mazza, J. Power Sources 178 (2008) 103–117.
[4] J. Goupy, L. Creighton, Introduction to Design of Experiments with JMP® Examples, third ed., SAS Publishing, Cary, NC, USA, 2007.
[5] D.C. Montgomery, Design and Analysis of Experiments, fifth ed., John Wiley & Sons, New York, 2001.
[6] H. Toutenburg, Statistical Analysis of Designed Experiments, second ed., Springer, New York, 2002.
[7] R.L. Mason, R.F. Gunst, J.L. Hess, Statistical Design and Analysis of Experiments with Applications to Engineering and Science, second ed., Hoboken, New Jersey, 2003.
[8] L. Eriksson, E. Johansson, N. Kettaneh-Wold, C. Wikström, S. Wold, Design of Experiments – Principles and Applications, 2000.
[9] B. Wahdame, D. Candusso, X. François, F. Harel, J.-M. Kauffmann, G. Coquery, Int. J. Hydrogen Energy 34 (2009) 967–980.
[10] O. Okur, Ç. İyigün Karadağ, F.G. Boyacı San, E. Okumuş, G. Behmenyar, Energy 57 (2013) 574–580.
[11] S. Endoo, K. Pruksathorn, P. Piumsomboon, Renew. Energy 35 (2010) 807–813.
[12] G. Velayutham, K.S. Dhathathreyan, N. Rajalakshmi, D. Sampangi Raman, J. Power Sources 191 (2009) 10–15.
[13] S. Flick, M. Schwager, E. McCarthy, W. Mérida, Appl. Energy 129 (2014) 135–146.
[14] F.G. Boyaci San, I. Isik-Gulsac, O. Okur, Energy 55 (2013) 1067–1075.
[15] S.-J. Cheng, J.-M. Miao, S.-J. Wu, Renew. Energy 39 (2012) 250–260.
[16] J.G. Carton, A.G. Olabi, Energy 35 (2010) 2796–2806.
[17] E.E. Kahveci, I. Taymaz, Int. J. Hydrogen Energy 39 (2014) 10655–10663.
[18] E. McCarthy, S. Flick, W. Mérida, J. Power Sources 239 (2013) 399–408.
[19] N. Hajjaji, V. Renaudin, A. Houas, M.N. Pons, Chem. Eng. Process. Process Intensif. 49 (2010) 500–507.
[20] M.F. Torchio, M.G. Santarelli, A. Nicali, J. Power Sources 149 (2005) 33–43.
[21] G.E.P. Box, H.L. Lucas, Biometrika 46 (1959) 77–90.
[22] P. Moçotéguy, B. Ludwig, N. Steiner, Int. J. Hydrogen Energy 39 (2014) 10230–10244.